Pramana – J. Phys. (2022) 96:51
https://doi.org/10.1007/s12043-021-02291-x

Nonlinear waves in electron–positron–ion plasmas including the full dynamics for all species

A MUGEMANA[1], S MOOLLA[2,*] and I J LAZARUS[2]

[1]School of Education, University of Rwanda, Rukara Campus, Butare, Rwanda
[2]Department of Mathematics, Statistics and Physics, Durban University of Technology, Durban 4000, South Africa
*Corresponding author. E-mail: sulemanm@dut.ac.za

MS received 26 April 2021; revised 6 September 2021; accepted 18 October 2021

Abstract. Nonlinear low-frequency electrostatic waves in a magnetised, three-component plasma consisting of warm electrons, warm positrons and cool ions have been investigated. The electrons, positrons and ions are governed by the fluid equations. The system is closed with the Poisson equation. This set of equations is numerically solved for the electric field. The effects of the driving electric field, ion temperature, densities, Mach number, propagation angle and drift velocity of different species are investigated. It is shown that depending on the driving electric field, temperature, densities, Mach number, propagation angle and drift velocity of different species on the nonlinear wave structures components, the numerical solutions exhibit waveforms that are sinusoidal, saw-tooth and spiky. The results are compared with satellite observations.

Keywords. Nonlinear waves; electrostatic waves; low frequency.

PACS Nos 52.35.Qz; 52.35.Fp; 52.35.Mw

1. Introduction

Observations made by different spacecrafts have established the presence of broadband electrostatic noise (BEN) in various regions of the Earth's magnetosphere. Several theoretical models have been introduced to explain the BEN detected in such environments. During these investigations, different researchers [1–5] considered magnetised plasma consisting of hot and cold species. The hot species were governed by the Boltzmann density distribution function and the cold species were governed by the fluid equations. They either used the quasi-neutrality condition or the Poisson equation to close their system of equations. Their results pointed out that the nonlinear coupling oscillations generate spiky structures with the period varying from ion-acoustic range to the ion cyclotron range [1,3].

Moolla *et al* [4] extended the work of Reddy *et al* [1] by including the Poisson equation. Their model was a three-component plasma consisting of cold electrons and cold ions, and hot electrons, where all species were governed by the fluid equations. They found that the nonlinear coupling between the high-frequency electron–cyclotron and electron-acoustic modes could explain the spiky structures in the high-frequency region of BEN.

Recently, Moolla *et al* [5] extended their previous high-frequency study by considering finite temperature effects. They investigated the pulse widths and periods of the waves and concluded that the ratio of the pulse widths to the periods of the electrostatic waves (ESW) is a constant. They also pointed out that with the inclusion of a finite cool electron temperature, the waves broadened and the nonlinearity enhanced.

In this paper, we explore the extension of the work of Mugemana *et al* [6], where all species are described by fluid equations and numerically solve the resulting set of coupled nonlinear equations. The organisation of this paper is as follows: In §2, we present the basic theory and model of the fluid equations governing the plasma dynamics. Based on appropriate initial conditions the numerical results and discussion are presented in §3. Finally, in §4, the results are briefly summarised.

2. Basic theory and model of fluid equations governing the plasma dynamics

We consider a collisionless, magnetised three-component plasma consisting of cool ions (i), warm positrons (p) and warm electrons (e) in the presence of an external magnetic field B_0 which is assumed to be in the

Published online: 20 February 2022

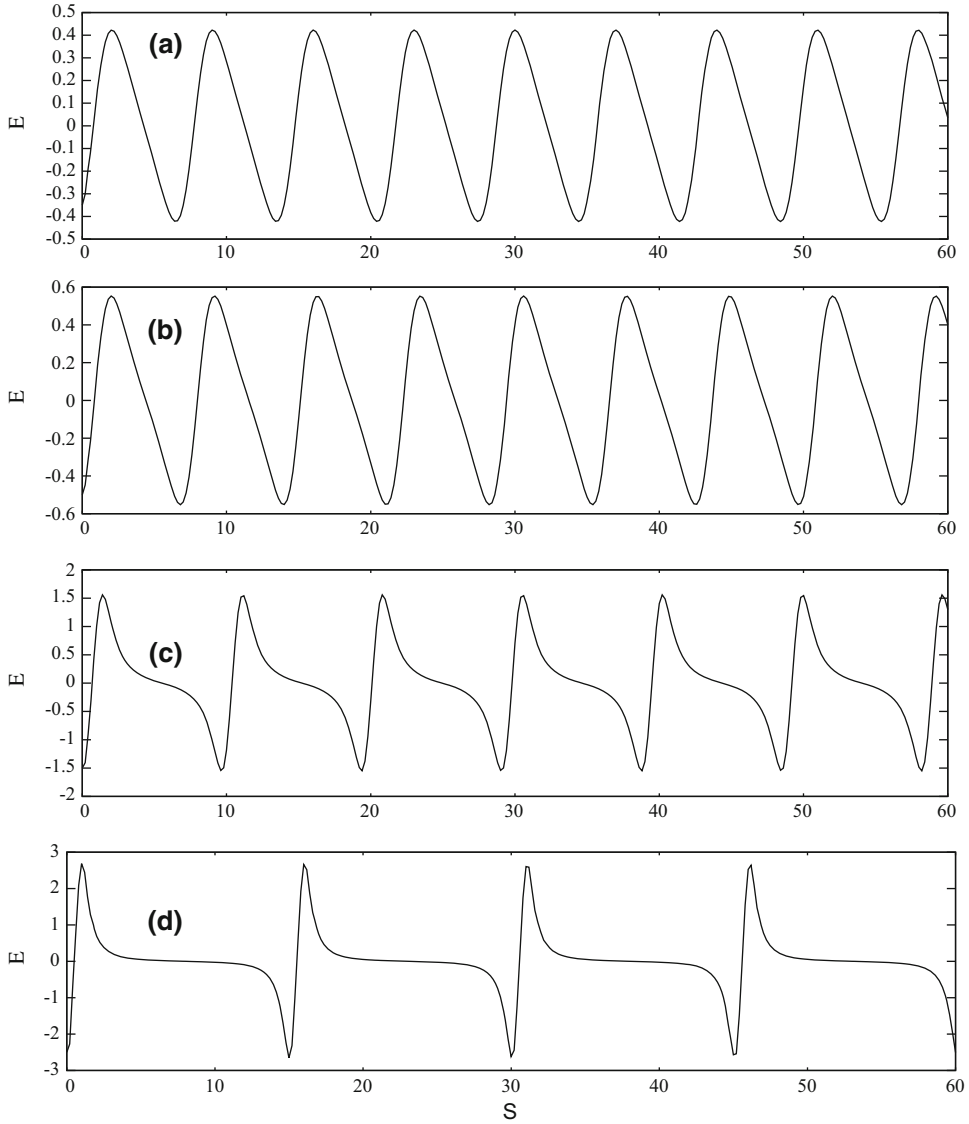

Figure 1. Numerical solution of the normalised parallel electric field for the parameters $M = 3.5$, $R = 5.0$, $\delta_i = \delta_e = \delta_p = 0.0$, $n_{i0}/n_{e0} = 0.5$, $n_{p0}/n_{e0} = 0.5$, $T_i/T_h = 0.0$, $\theta = 2°$ for (**a**) $E_0 = 0.35$, (**b**) $E_0 = 0.5$, (**c**) $E_0 = 1.5$ and (**d**) $E_0 = 2.5$.

x–z plane and making an angle θ with the x-axis. The basic equations, governing the dynamical system, are the equations of continuity and momentum which are written as

$$\frac{\partial n_j}{\partial t} + \frac{\partial n_j v_{jx}}{\partial x} = 0, \tag{1}$$

$$\frac{\partial v_{jx}}{\partial t} + v_{jx}\frac{\partial v_{jx}}{\partial x} + \frac{1}{n_j m_j}\frac{\partial p_j}{\partial x} = -\frac{\varepsilon_j e}{m_i}\frac{\partial \varphi}{\partial x} + \varepsilon_j \Omega_j v_{jy}\sin\theta, \tag{2}$$

$$\frac{\partial v_{jy}}{\partial t} + v_{jx}\frac{\partial v_{jy}}{\partial x} = \varepsilon_j \Omega_j v_{jz}\cos\theta - \varepsilon_j \Omega_j v_{jx}\sin\theta, \tag{3}$$

$$\frac{\partial v_{jz}}{\partial t} + v_{jx}\frac{\partial v_{jz}}{\partial x} = -\varepsilon_j \Omega_j v_{jy}\cos\theta, \tag{4}$$

$$\frac{\partial p_j}{\partial t} + v_{jx}\frac{\partial p_j}{\partial x} + 3p_j\frac{\partial v_{jx}}{\partial x} = 0. \tag{5}$$

Equations (1)–(5) are closed with the Poisson equation

$$\varepsilon_0\frac{\partial^2 \varphi}{\partial x^2} = -e(n_p - n_e + n_i). \tag{6}$$

In eqs (1)–(6), $\varepsilon_j = -1(1)$ for $j = e(i, p)$, $\Omega_j = eB_0/m_j$ is the ion (electron) cyclotron frequency for $j = i(e, p)$, n_j is the density of the jth species, v_{jx}, v_{jy} and v_{jz} are the components of the velocity of the j species along the x, y and z directions.

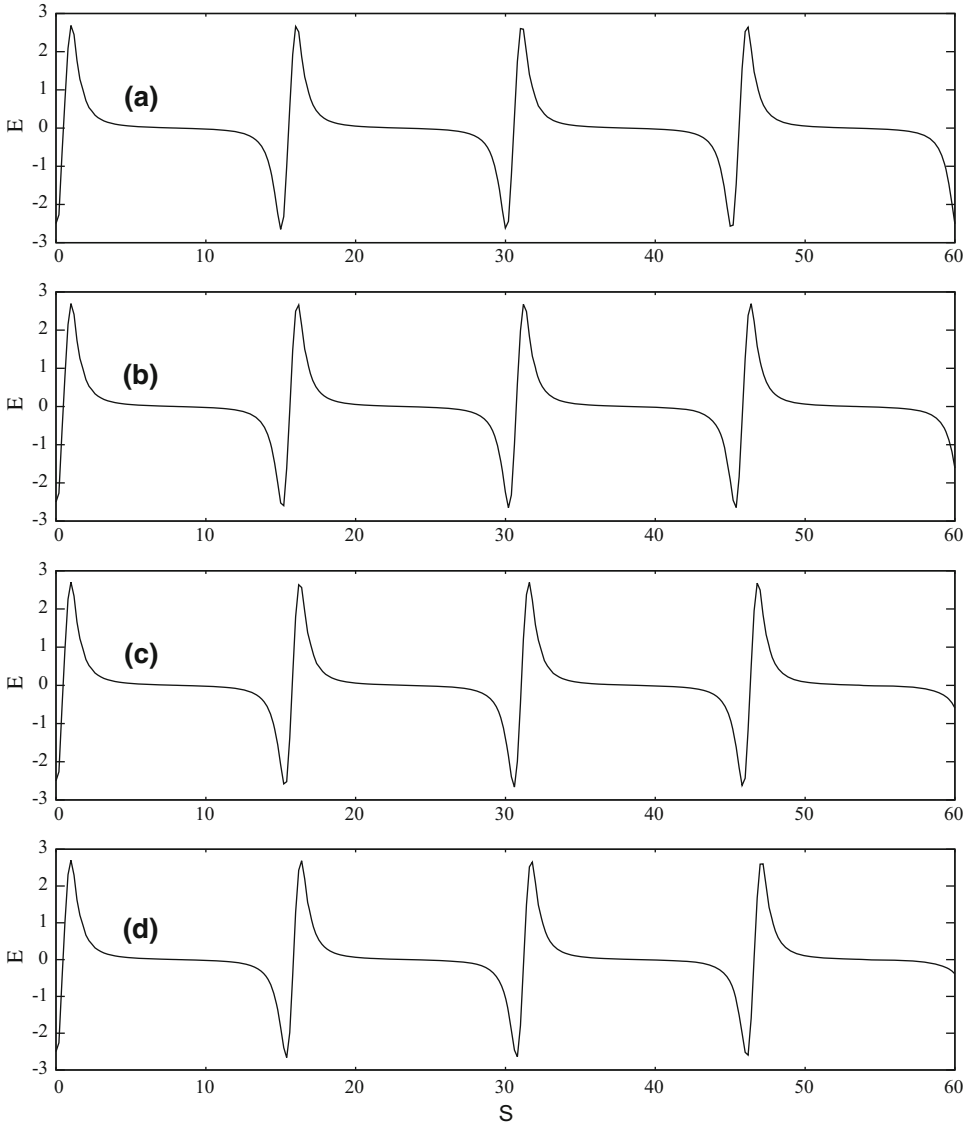

Figure 2. Numerical solution of the normalised parallel electric field for the parameters $E_0 = 2.5$, $M = 3.5$, $R = 5.0$, $\delta_i = \delta_e = \delta_p = 0.0$, $n_{i0}/n_{e0} = 0.5$, $n_{p0}/n_{e0} = 0.5$, $\theta = 2$ for (**a**) $T_i/T_h = 0.0$, (**b**) $T_i/T_h = 0.05$, (**c**) $T_i/T_h = 0.15$ and (**d**) $T_i/T_h = 0.2$.

2.1 *Nonlinear analysis*

For the nonlinear analysis, the new physical stretch variable depending on t and v is introduced. We transform eqs (1)–(6) to a stationary frame using $s = (x - vt)/(v/\Omega_i)$ and normalise velocities with respect to the ion thermal velocity $C_s = \sqrt{T_i/m_i}$, with T_i being the ion temperature and m_i being the ion mass; densities with respect to the total unperturbed electron density n_{e0}; pressures with respect to $n_{e0}T_h$ and electrostatic wave potential normalised to T_h/e, with T_h being the electron temperature and e being the magnitude of the electron charge. We replace $\partial/\partial t$ by $-\Omega_i(\partial/\partial s)$ and $\partial/\partial x$ by $(\Omega_i/v)(\partial/\partial s)$ in eqs (1)–(6) and define the normalised electric potential $\psi = e\varphi/T_h$ and electric field $E = -(\partial\psi/\partial s)$. We use the following initial conditions: $\psi = 0$, $\partial\psi/\partial s = E_0$, $\partial^2\psi/\partial s^2 = 0$, $n_j = n_{j0}$ and $V_{jx} = v_{j0}\cos\theta$ at $s = 0$. In addition, we assume point quasineutrality, i.e., $n_{i0} + n_{p0} = n_{e0}$ at equilibrium. The results obtained are expressed as a set of differential equations given below:

$$\frac{\partial\psi}{\partial s} = -\tilde{E} \tag{7}$$

$$\frac{\partial\tilde{E}}{\partial s} = M^2R^2\frac{n_{e0}}{n_{i0}}(\tilde{n}_p + \tilde{n}_i - \tilde{n}_e) \tag{8}$$

$$\frac{\partial\tilde{n}_e}{\partial s} = \frac{\tilde{n}_e^3[\tilde{E} + \frac{m_i}{m}M\tilde{v}_{ey}\sin\theta]}{(M - \delta_e)^2 - 3\tilde{n}_e\tilde{P}_e} \tag{9}$$

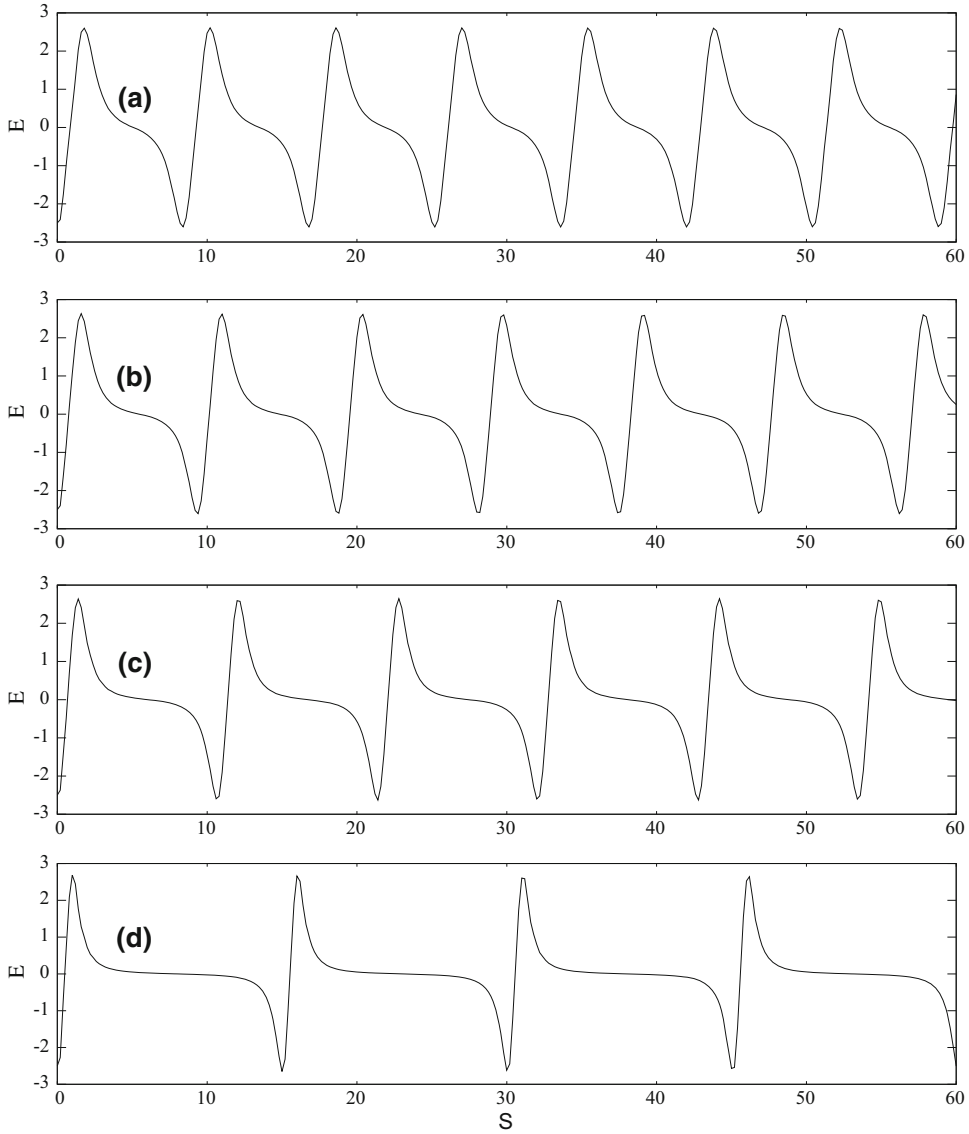

Figure 3. Numerical solution of the normalised parallel electric field for the parameters $E_0 = 2.5$, $M = 3.5$, $R = 5.0$, $\delta_i = \delta_e = \delta_p = 0.0$, $n_{p0}/n_{e0} = 0.5$, $\theta = 2°$, $T_i/T_h = 0.0$ for (**a**) $n_{i0}/n_{e0} = 0.7$, (**b**) $n_{i0}/n_{e0} = 0.65$, (**c**) $n_{i0}/n_{e0} = 0.6$ and (**d**) $n_{i0}/n_{e0} = 0.5$.

$$\frac{\partial \tilde{P}_e}{\partial s} = \frac{3\tilde{P}_e\tilde{n}_e^2[\tilde{E} + \frac{m_i}{m}M\tilde{v}_{ey}\sin\theta]}{(M-\delta_e)^2 - 3\tilde{n}_e p_{\tilde{P}e}} \tag{10}$$

$$\frac{\partial \tilde{v}_{ey}}{\partial s} = \left(\frac{m_i}{m}\right)\frac{\tilde{n}_e M}{(M-\delta_e)}\left[\tilde{v}_{ez}\cos\theta - M\sin\theta\right] + \left(\frac{m_i}{m}\right)M\sin\theta \tag{11}$$

$$\frac{\partial \tilde{v}_{ez}}{\partial s} = -\left(\frac{m_i}{m}\right)\frac{n_{en}M\tilde{v}_{ey}\cos\theta}{(M-\delta_e)} \tag{12}$$

$$\frac{\partial \tilde{n}_p}{\partial s} = \frac{\tilde{n}_p^3[-\tilde{E} - \frac{m_i}{m}M\tilde{v}_{py}\sin\theta]}{\left(\frac{n_{p0}}{n_{e0}}\right)^2(M-\delta_p)^2 - 3\left(\frac{n_{p0}}{n_{e0}}\right)\tilde{n}_p\tilde{P}_p} \tag{13}$$

$$\frac{\partial \tilde{P}_p}{\partial s} = \frac{3\tilde{P}_p\tilde{n}_p^2[-\tilde{E} - \frac{m_i}{m}M\tilde{v}_{py}\sin\theta]}{\left(\frac{n_{p0}}{n_{e0}}\right)^2(M-\delta_p)^2 - 3\left(\frac{n_{p0}}{n_{e0}}\right)\tilde{n}_p\tilde{P}_p} \tag{14}$$

$$\frac{\partial \tilde{v}_{py}}{\partial s} = \left(\frac{m_i}{m}\right)\left(\frac{n_{e0}}{n_{p0}}\right)\frac{\tilde{n}_p M}{(M-\delta_p)}[M\sin\theta - \tilde{v}_{pz}\cos\theta] - \left(\frac{m_i}{m}\right)M\sin\theta \tag{15}$$

$$\frac{\partial \tilde{v}_{pz}}{\partial s} = \left(\frac{m_i}{m}\right)\frac{\tilde{n}_p M\tilde{v}_{ey}\cos\theta}{(M-\delta_p)} \tag{16}$$

$$\frac{\partial \tilde{n}_i}{\partial s} = \frac{\tilde{n}_i^3[-\tilde{E} - M\tilde{v}_{iy}\sin\theta]}{\left(\frac{n_{i0}}{n_{e0}}\right)^2(M-\delta_i)^2 - 3\tilde{n}_i\tilde{P}_i} \tag{17}$$

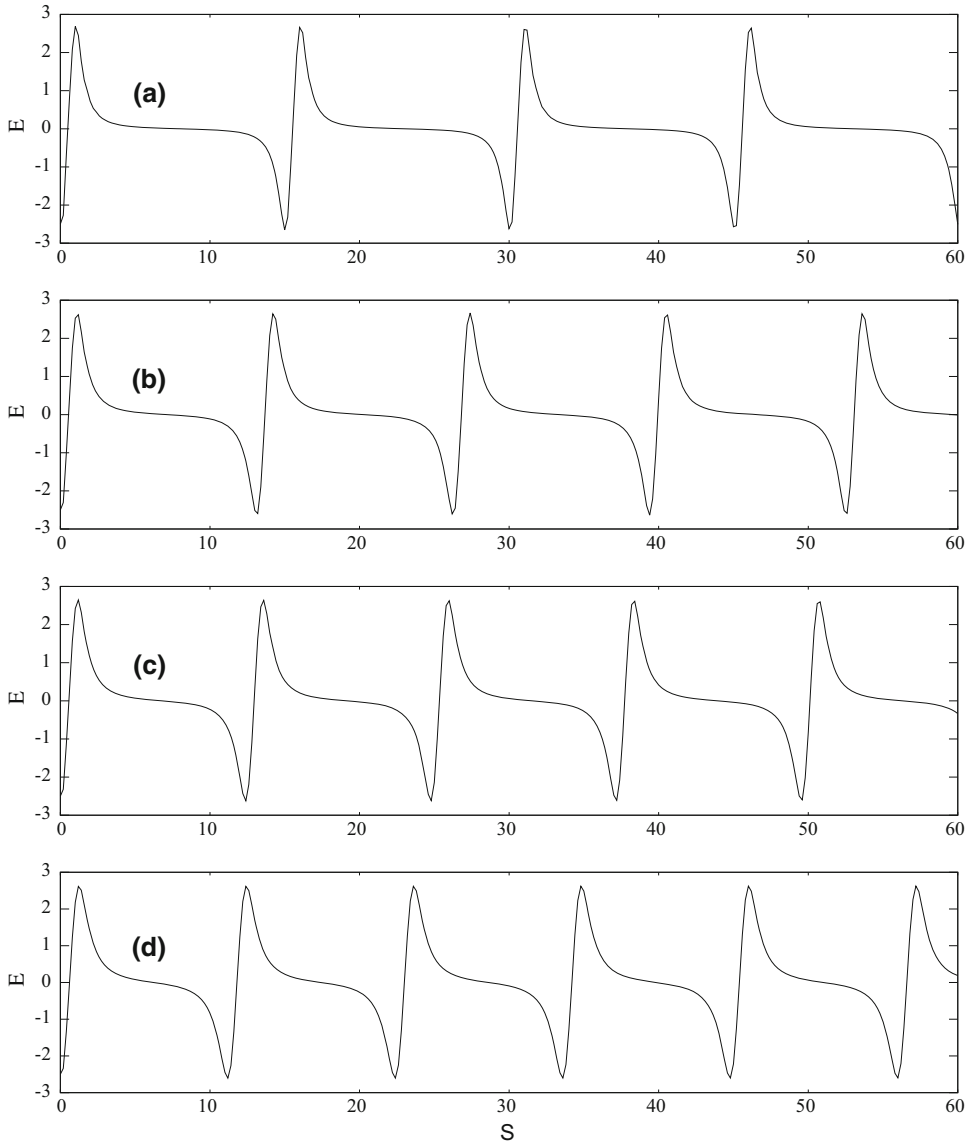

Figure 4. Numerical solution of the normalised parallel electric field for the parameters $E_0 = 2.5$, $R = 5.0$, $\delta_i = \delta_e = \delta_p = 0.0$, $\theta = 2°$, $T_i/T_h = 0.0$, $n_{p0}/n_{e0} = n_{i0}/n_{e0} = 0.5$ for (**a**) $M = 3.5$, (**b**) $M = 3.7$, (**c**) $M = 3.8$ and (**d**) $M = 4.0$.

$$\frac{\partial \tilde{P}_i}{\partial s} = \frac{3\tilde{P}_i\tilde{n}_i^2[-\tilde{E} - M\tilde{v}_{iy}\sin\theta]}{\left(\frac{n_{i0}}{n_{e0}}\right)^2 (M-\delta_i)^2 - 3\tilde{n}_i\tilde{P}_i} \tag{18}$$

$$\frac{\partial \tilde{v}_{iy}}{\partial s} = \frac{\tilde{n}_i M}{\left(\frac{n_{i0}}{n_{e0}}\right)(M-\delta_i)}\left[M - \tilde{v}_{iz}\cos\theta\right] - M\sin\theta \tag{19}$$

$$\frac{\partial \tilde{v}_{iz}}{\partial s} = \frac{\tilde{n}_i M\tilde{v}_{iy}\cos\theta}{\left(\frac{n_{i0}}{n_{e0}}\right)(M-\delta_i)}, \tag{20}$$

where m is the mass of the electrons/positrons, $\delta_j = v_{j0}/C_s$ is the normalised flow velocity of the jth species, $M = v/C_s$ is the Mach number and $R = \omega_{pi}/\Omega_i$. The additional superscript '$\sim$' introduced in eqs (7)–20) indicates normalised quantities.

3. Numerical results and discussion

The set of nonlinear differential equations (7)–(20) is solved numerically using the Runge–Kutta method. The initial values of $\tilde{v}_{ey}, \tilde{v}_{ez}, \tilde{v}_{py}, \tilde{v}_{pz}$ are given but $\tilde{v}_{iy0}$ and $\tilde{v}_{iz0}$ are calculated self-consistently. We shall investigate the effects of driving amplitude, temperature, densities, Mach number, propagation angle and drift velocity of different species on the nonlinear wave structures.

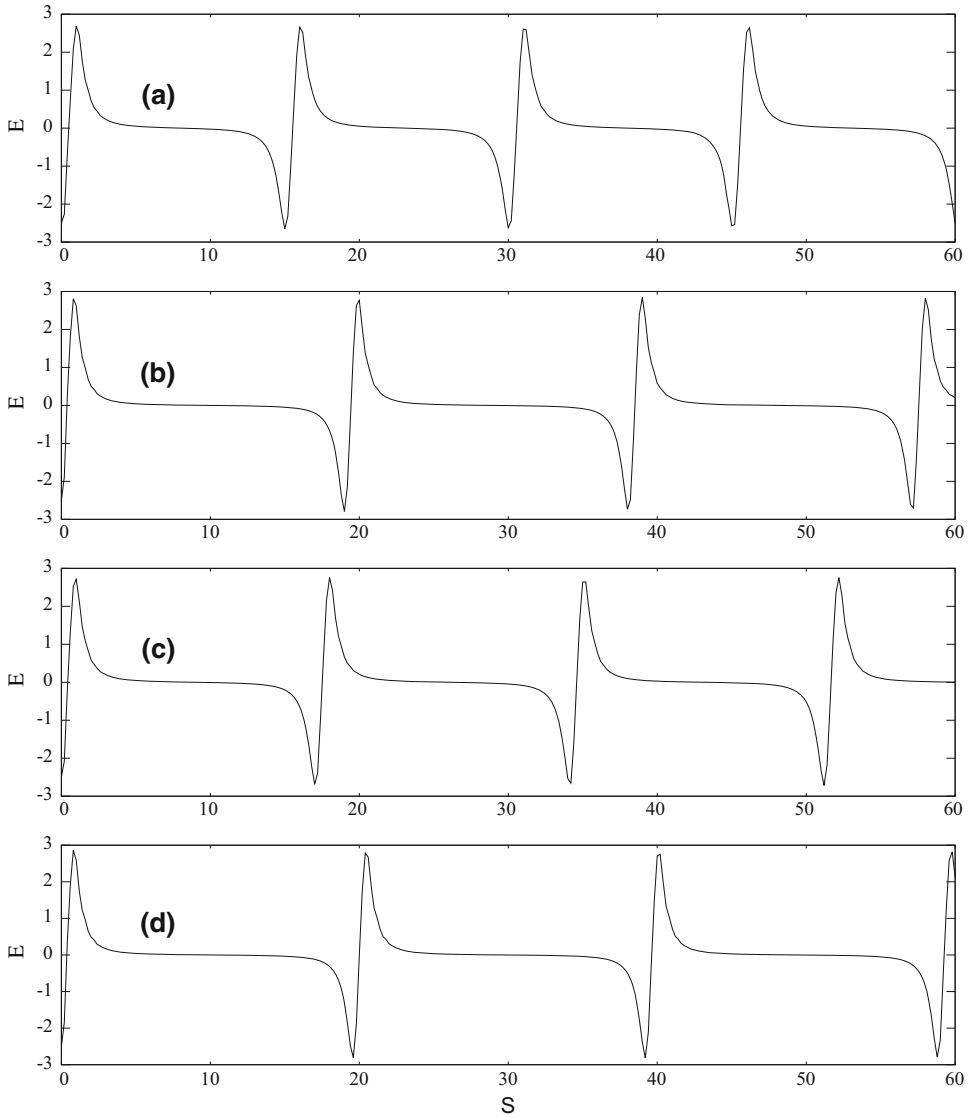

Figure 5. Numerical solution of the normalised parallel electric field for the parameters $E_0 = 2.5$, $M = 3.5$, $R = 5.0$, $\delta_i = \delta_e = \delta_p = 0.0$, $T_i/T_h = 0.0$, $n_{p0}/n_{e0} = n_{i0}/n_{e0} = 0.5$ for (**a**) $\theta = 2°$, (**b**) $\theta = 6°$, (**c**) $\theta = 10°$ and (**d**) $\theta = 15°$.

3.1 *Effect of driving electric field* E_0

For the fixed parameters $M = 3.5$, $\delta_e = \delta_p = \delta_i = 0.0$, $n_{i0}/n_{e0} = 0.5$, $T_i/T_h = 0.0$, $R = 5.0$ and $\theta = 2°$, we vary the driving electric field E_0 from 0.35 to 2.5. The results are presented in figure 1. This figure shows that by increasing E_0, the period of oscillations increases from $1.12\tau_{ci}$ to $2.43\tau_{ci}$, where $\tau_{ci} = 2\pi/\Omega_i$ is the ion cyclotron period. We observe a transition from ion-cyclotron waves to ion-acoustic waves as the electric field structures evolve from a sinusoidal waveform to a saw-tooth structure. The present plasma model can generate spiky structures for a minimum driving field $E_0 = 0.35$, while the plasma models investigated by Bharuthram *et al* [3] and Moolla *et al* [7] required driving field strength 1.1 and 0.3 respectively for the onset of spikes. Comparing these results with those obtained by Mugemana *et al* [6], we observe the increase in the driving field for the onset of spikes from 0.01 for the Boltzmann density distribution to 0.35 for full dynamical system, while the value of R increases from 3 to 5.

3.2 *Effect of the temperature ratio* T_i/T_h

Figure 2 shows the effect of ion-electron temperature ratio T_i/T_h on the parallel electric field structures for the fixed parameters, $M = 3.50$, $E_0 = 2.5$, $\delta_e = \delta_p = \delta_i = 0.0$, $n_{i0}/n_{e0} = 0.5$, $R = 5.0$ and $\theta = 2°$. The variation of the ion-electron temperature ratio does not affect the nonlinearity of the waves and the wave structures are spiky in nature [7]. However, increasing this ratio from

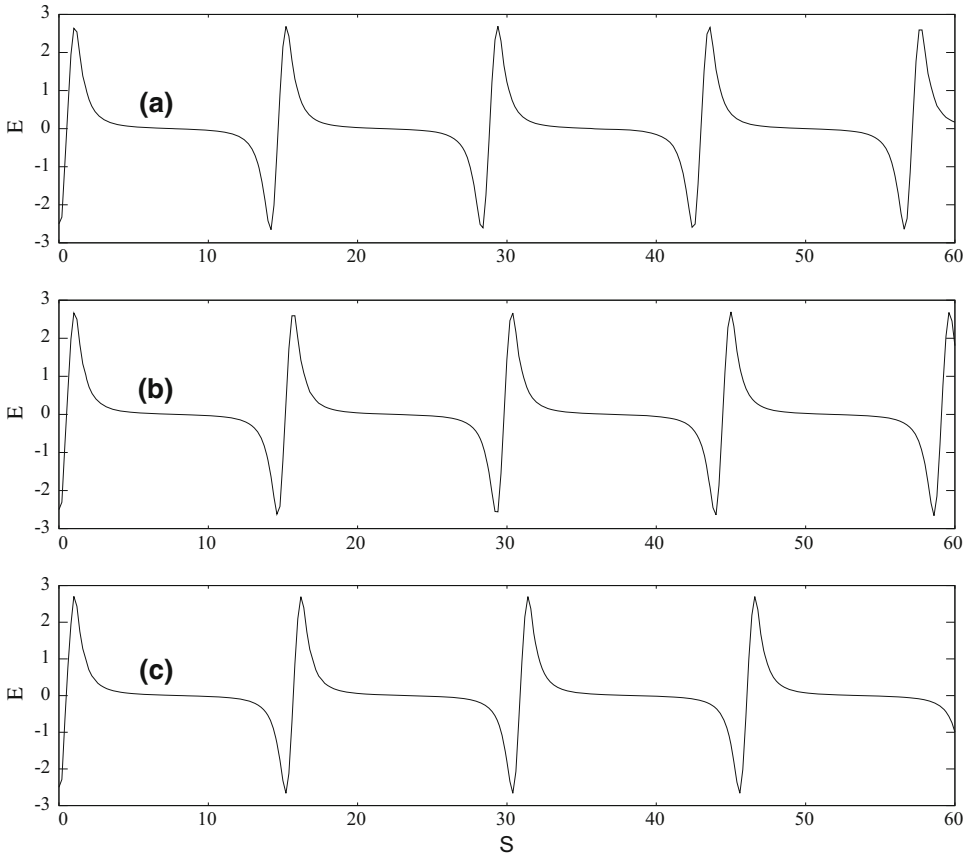

Figure 6. Numerical solution of the normalised parallel electric field for the parameters $E_0 = 2.5$, $M = 3.5$, $R = 5.0$, $\delta_i = \delta_p = 0.0$, $\theta = 2°$, $T_i/T_h = 0.5$, $n_{p0}/n_{e0} = n_{i0}/n_{e0} = 0.5$ for (**a**) $\delta_e = -0.10$, (**b**) $\delta_e = 0.0$ and (**c**) $\delta_e = 0.10$.

0.0 to 0.2 results in the increase in the period of the waves from $2.43\tau_{ci}$ to $2.57\tau_{ci}$ because dispersive effect causes the broadening of the waves.

3.3 *Effect of density ratio* n_{p0}/n_{e0}

Figure 3 illustrates the effect of positron density on the parallel electric field structures for the following fixed parameters: $M = 3.5$, $E_0 = 2.5$, $\delta_e = \delta_p = \delta_i = 0.0$, $R = 5.0$ and $\theta = 2°$. It is seen that as n_{p0}/n_{e0} increases from 0.3 to 0.5, the waveforms become more nonlinear and the period of these waveforms increases from $1.31\tau_{ci}$ to $2.43\tau_{ci}$. The increase in positron densities enhances nonlinearity, making spiky structures easier to generate. These results are similar to those of [7].

3.4 *Effect of Mach number M*

Figure 4 presents the effect of Mach number on the parallel electric field structures for the fixed parameters, $E_0 = 2.5$, $\delta_e = \delta_p = \delta_i = 0.0$, $n_{p0}/n_{e0} = n_{i0}/n_{e0} = 0.5$, $R = 5.0$ and $\theta = 2°$. It is seen that as the Mach number increases from 3.5 to 4.0, the period of these waveforms increases from $2.38\tau_{ci}$ to $2.43\tau_{ci}$. Our studies showed that the value of M needs to be in a narrow range for the electric field structures to exist. Hence, varying the values of M in this range shows slight effect on the waves. These results are similar to those of [5].

3.5 *Effect of propagation angle* θ

Figure 5 illustrates the effect of propagation angle on the parallel electric field structures for the fixed parameters, $E_0 = 2.5$, $\delta_e = \delta_p = \delta_i = 0.0$, $n_{p0}/n_{e0} = n_{i0}/n_{e0} = 0.5$, $R = 5.0$ and $M = 3.5$. We vary the propagation angle from $\theta = 0°$ to $15°$. This results in increasing the period of oscillations from $2.38\tau_{ci}$ to $3.18\tau_{ci}$. It is seen that there is a decrease in frequency with no effect on nonlinearity. In this study, the maximum propagation angle is approximately $15°$. Beyond this value, our model does not present the waveforms similar to those observed by Matsumoto *et al* [8]. The assumption of Reddy *et al* [1] and Moolla *et al* [5] showing that the angle of wave propagation with the Earth's magnetic field may be set to two degree ($\theta = 2°$) during investigation of electrostatic waves in Earth's magnetosphere remains reasonable.

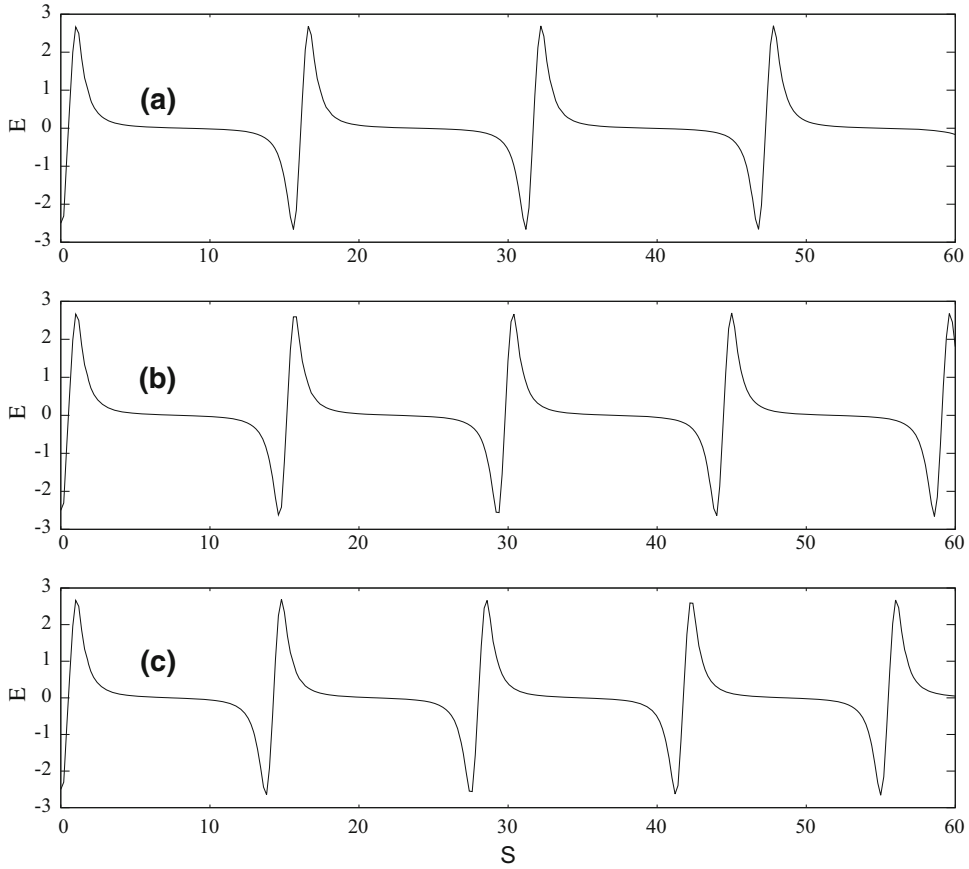

Figure 7. Numerical solution of the normalised parallel electric field for the parameters $E_0 = 2.5$, $M = 3.5$, $R = 5.0$, $\delta_e = \delta_p = 0.0$, $\theta = 2°$, $T_i/T_h = 0.5$, $n_{p0}/n_{e0} = n_{i0}/n_{e0} = 0.5$ for (**a**) $\delta_i = -0.10$, (**b**) $\delta_i = 0.0$ and (**c**) $\delta_i = 0.10$.

3.6 *Effect of electron drift*

The effect of electron drift velocity on the electric field structures for the fixed parameters, $E_0 = 2.5$, $M = 3.5$, $R = 5.0$, $\theta = 2°$, $T_i/T_h = 0.0$, $\delta_i = \delta_p = 0.0$ and $n_{p0}/n_{e0} = n_{i0}/n_{e0} = 0.5$, are depicted in figure 6. It is seen that for the antiparallel electron drifts ($\delta_e < 0$), the periods of the waves are significantly lower than that for the parallel drifts ($\delta_e > 0$). Consequently, the period of the waves increases from $2.25\tau_{ci}$ for $\delta_e = -0.10$ to $2.45\tau_{ci}$ for $\delta_e = 0.10$. However, the nonlinearity is unaffected and all waveforms are spiky in nature. Similar results have been reported by Moolla *et al* [5] during an investigation of the effect of the cool electron drift.

3.7 *Effect of ion drift*

The effect of ion drift velocity on the electric field structures is presented in figure 7 for the fixed parameters, $E_0 = 2.5$, $M = 3.5$, $R = 5.0$, $\theta = 2°$, $T_i/T_h = 0.0$, $\delta_e = \delta_p = 0.0$ and $n_{p0}/n_{e0} = n_{i0}/n_{e0} = 0.5$. It is seen that for the antiparallel ion drift ($\delta_i < 0$), the periods of the waves are significantly higher than that for the parallel drift ($\delta_i > 0$). From antiparallel to parallel drifts, the period of spikes decreases from $2.52\tau_{ci}$ for $\delta_i = -0.10$ to $2.19\tau_{ci}$ for $\delta_i = 0.10$. However, the nonlinearity is unaffected and all waveforms are spiky in nature. These results are similar to those of Moolla *et al* [7] and are in agreement with the satellite observations showing that the period of the spiky structures vary rapidly due to the drifting particles being accelerated in bursts [4].

3.8 *Effect of positron drift*

We investigate the effect of positron drift velocity on the electric field structures as shown in figure 8 for the fixed parameters, $E_0 = 2.5$, $M = 3.5$, $R = 5.0$, $\theta = 2°$, $T_i/T_h = 0.0$, $\delta_i = \delta_e = 0.0$ and $n_{p0}/n_{e0} = n_{i0}/n_{e0} = 0.5$. It is seen that for antiparallel positron drift ($\delta_p < 0$), the period of the waves is significantly lower than that for the parallel drift ($\delta_p > 0$). From

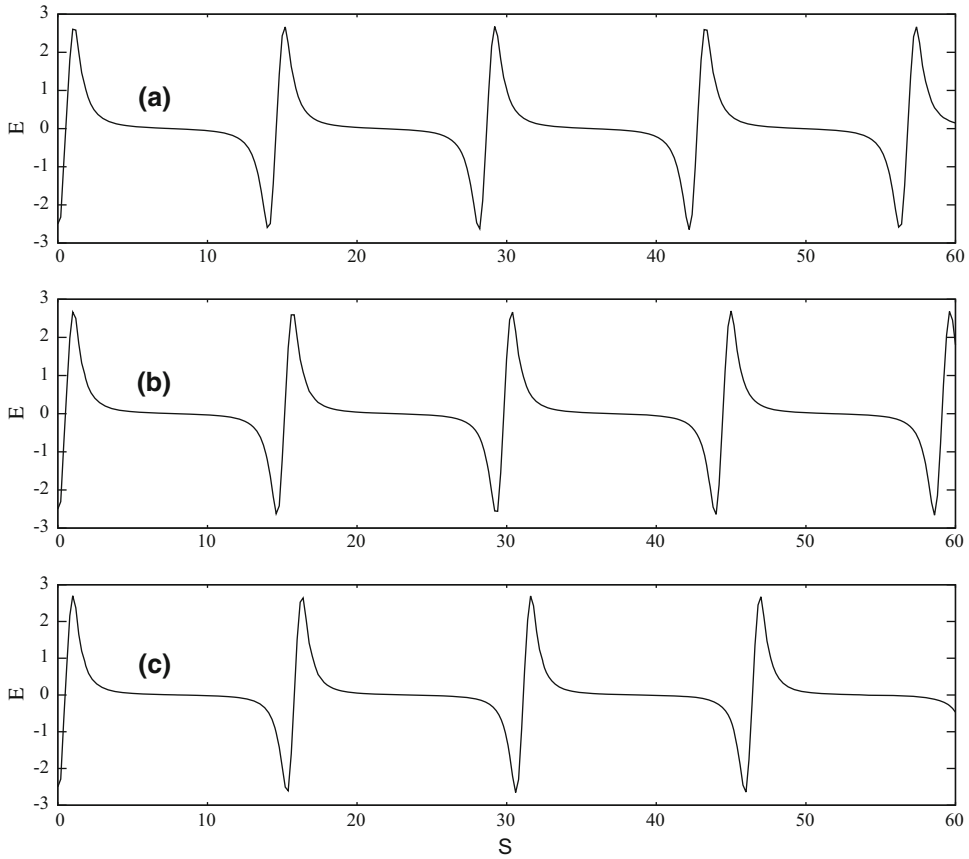

Figure 8. Numerical solution of the normalised parallel electric field for the parameters $E_0 = 2.5$, $M = 3.5$, $R = 5.0$, $\delta_e = \delta_i = 0.0$, $\theta = 2°$, $T_i/T_h = 0.5$, $n_{p0}/n_{e0} = n_{i0}/n_{e0} = 0.5$ for (**a**) $\delta_p = -0.10$, (**b**) $\delta_p = 0.0$ and (**c**) $\delta_p = 0.10$.

antiparallel to parallel drift, the frequency of electrostatic waves decreases, i.e. the period of spikes increases from $2.25\tau_{ci}$ for $\delta_p = -0.10$ to $2.45\tau_{ci}$ for $\delta_p = 0.10$. However, the nonlinearity is unaffected and all waveforms are spiky in nature. The behaviour of the spiky electric field is similar to that of the electron drift. We note that the period of the spiky structures for positrons and electrons drift increases from antiparallel to parallel drifts, while, in the case of the ion drift velocity δ_i, the opposite trend occurs.

4. Summary

We have studied nonlinear low-frequency waves in an e–p–i plasma whereby this model is treated using full dynamics for all three species. The effects of the driving electric field, ion temperature, positron density, Mach number, propagation angle and drift velocity on each component were studied. The findings show that the electric field structures vary from sinusoidal to saw-tooth to spiky waveforms, confirming the results of Bharuthram *et al* [9] attesting that the nonlinear waves evolve in a consistent fashion irrespective of the plasma composition. Thus, the correlation between the ESWs generated and broadband electrostatic noise from the satellite data is strong [10]. The results of our analysis can be applied to similar environments generally found around other solar and extra-solar planetary bodies.

References

[1] R V Reddy, G S Lakhina, N Singh and R Bharuthram, *Nonlinear Process Geophys*. **9**, 25 (2002)
[2] R V Reddy, S V Singh, G S Lakhina and R Bharuthram, *Earth Planets Space* **58**, 1227 (2006)
[3] R Bharuthram, R V Reddy, G S Lakhina and N Singh, *Phys. Scr*. **98**, 137 (2002)
[4] S Moolla, R Bharuthram, S V Singh and G S Lakhina, *Pramana – J. Phys.* **61**, 1209 (2003)
[5] S Moolla, R Bharuthram, S V Singh, G S Lakhina and R V Reddy, *J. Geophys. Res*. **112**, A07214 (2007)

[6] A Mugemana, S Moolla and I J Lazarus, *Pramana – J. Phys*. **88**, 22 (2017)
[7] S Moolla, I J Lazarus and R Bharuthram, *J. Plasma Phys*. **78**, 545 (2012)
[8] H H Matsumoto, T Kojima, Y Miyatake, M Omura, I Okada, Nagano and M Tsutsui, *Geophys. Res. Lett*. **21**, 2915 (1994)
[9] R Bharuthram, S V Singh, S K Maharaj, S Moolla, I J Lazarus, R V Reddy and G S Lakhina, *J. Plasma Phys*. **80**, 825 (2014)
[10] R E Ergun, C W Carlson, J P McFadden, F S Mozer, G T Delroy, W Peria, C C Chaston, M Temerin, R Elphic, R Strangeway, R C Pfaff, A Cattell and A Cattell, *Geophys. Res. Lett.* **25**, 2025 (1998)